Heat Mass Transfer (2005) 41: 667–673
DOI 10.1007/s00231-004-0609-2

ORIGINAL

X. M. Huang · W. Liu · A. Nakayama · S. W. Peng

Modeling for heat and mass transfer with phase change in porous wick of CPL evaporator

Received: 20 October 2004 / Accepted: 25 October 2004 / Published online: 4 March 2005

A mathematic model is developed to describe heat and mass transfer with phase change in the porous wick of evaporator of capillary pumped loop (CPL). This model with six field variables, including temperature, liquid content, pressure, liquid velocity, vapor velocity and phase-change rate, is closed mathematically with additional pressure relationships introduced. The present model is suitable to the numerical computation, as the established equations become comparatively easy to solve, which is applied to CPL evaporator. The numerical results are obtained and the parameter effects on evaporator are discussed. The study demonstrates that instead of an evaporative interface, there exists an unsaturated two-phase zone between the vapor-saturated zone and the liquid-saturated zone in the wick of CPL evaporator.

Keywords CPL evaporator · Porous wick · Phase change · Heat and mass transfer · Numerical analysis

Nomenclature

c	Specific heat, J/(KgK)
k	Thermal conductivity, W/(mK)
k_v	Equivalent permeability of vapor, m^2
k_l	Unsaturated permeability of liquid, m^2
K_v	Infiltrating conductivity of vapor, ms^{-1}
K_l	Hydraulic conductivity of liquid, ms^{-1}
$\dot{m}$	mass rate of phase change, $Kg/(m^3s)$
P	Pressure, Pa
q	Heat flux, Wm^{-2}
Q	Heat load of the evaporator, W
S	Source term, saturation
t	Time, s
T	Temperature, K(°C)
u	Velocity component in x-direction, ms^{-1}
v	Velocity component in y-direction, ms^{-1}
$\vec{V}$	Velocity vector, ms^{-1}

Greek symbols

γ	Latent heat, JKg^{-1}
ε	Phase content, %
μ	Viscosity, Kg/(ms)
υ	Kinematic viscosity, m^2s^{-1}
ρ	Density, Kgm^{-3}
ω	Porosity, %

Subscripts

eff	Effective quantities
l	Liquid
s	Solid
v	Vapor

X. M. Huang · W. Liu (✉) · S. W. Peng
School of Energy and Power Engineering,
Huazhong University of Science and Technology,
Wuhan, 430074, People's Republic of China
E-mail: w_liu@hust.edu.cn
Tel.: +86-27-87541998
Fax: +86-27-87540724

A. Nakayama
Department of Mechanical Engineering,
Shizuoka University, 3-5-1 Johoku,
Hamamatsu, 432-8561, Japan

1 Introduction

Evaporators capable of transferring high heat fluxes (for example, as high as 100 W cm^{-2}) are of great interest for cooling of electronic components. A promising design for the evaporator is applied to capillary pumped loop (CPL), which has been advanced in recent 20 years (Fig. 1). The advantage of a CPL system is that it needs no power to operate and can transfer heat over distance as long as 30 foot or more. Since heat is transferred along with evaporation and condensation, a CPL is much more economical in terms of weight than conventional heat systems, which is very important for the application in

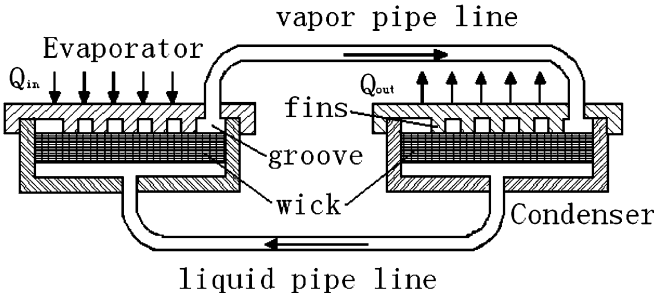

Fig. 1 Schematic of a system of CPL

the thermal control for satellite, spacecraft and space-platform.

Though the CPL has the potential as a heat transfer system with high efficiency, some technical problems remain unsolved. The primary concern is their reliability. It has been proven that the CPL is not very reliable in the space operation and the explanation for this has been elusive. Another problem is that the CPL requires a lengthy start-up procedure and the start-ups are not always successful. To analyze the phenomena, the physical process in the CPL evaporator should be investigated, either experimentally or numerically.

The main difficulty to evaluate heat transfer in such a system is lack of understanding for multiphase interactions in unsaturated porous media. For the majority of porous materials, the pore dimensions are small, which accentuates the interfacial tension effects. The experiment is also difficult to obtain data on system variables, such as individual phase pressure, liquid–vapor interfacial geometry, and fluid velocities on the pore level. The pore geometry is extremely complex, which necessitates the macroscopic averaging of microscopic phenomena. These make the experimental approach almost impossible.

Although experimental data on the present topic is scarce, some relevant theoretical and numerical investigations had been reported in the literature. Cao and Faghri [1] developed an analytical solution for heat and mass transfer processes during evaporation in the wick of a CPL evaporator. The model is strictly limited to a homogeneous porous wicks completely saturated by liquid. In their later study, Cao and Faghri [2] presented a conjugate analysis for a system including a segment of wick and a vapor groove. In particular, the influence of working fluid property on vapor flow in groove was studied. Again, evaporation is taken to only occur at the groove-wick interface. Khrusalev and Faghri [3] numerically investigated a similar configuration. They formulated the problem based on two important assumptions. First, there existed a superheated vapor zone in the vicinity of heated wall while the wick was saturated by sub-cooling liquid elsewhere. Based on this assumption, Darcy's law was applied to the vapor zone and the liquid zone, respectively. Second, when the vapor zone did not exceed the heated surface, there would be liquid meniscus on the top of porous surface. On the other hand, when the vapor zone extended beyond the surface of the heated wall, this liquid meniscus would disappear and the critical heat flux was reached.

In the work mentioned above, a common assumption is usually made as that the evaporation takes place only at the interface between vapor-saturated region and liquid-saturated region, and the interface thickness is zero, which implies that there are two single-phase regions in the wick: the vapor zone and the liquid zone. However, different results have also been reported in such a structure with phase change. A two-phase zone is observed between liquid and vapor saturated zones [4]. Udell [5] developed a numerical model to predict the length of this zone as a function of the heat flux, fluid properties, and porous medium characteristics. Zhao and Liao [6, 7] developed an experimental structure to study the characteristics of capillary-driven flow and phase-change heat transfer. Their study shows that for small and moderate heat fluxes, the whole porous structure was fully saturated with liquid except adjacent to horizontal heated surface where evaporation took place uniformly. For higher heat fluxes, a two-phase zone developed in the upper portion of the porous structure while the lower portion of the porous structure was saturated with sub-cooling liquid. When the imposed heat flux is further increased, a vapor blanket is formed below the heated surface and the corresponding critical heat flux is reached.

As we known that the capillary force results from the surface tension on meniscus. Under steady-state conditions, the meniscus of liquid perfectly wetting a solid surface extends as a liquid thin film over the solid surface. The thickness of this liquid film is dependent on physical properties of liquid and solid as well as surface tension related to temperature. The surface tension, thereby the liquid film thickness, decreases with the increase of temperature. This implies that surface tension gradient exists and liquid content gradient occurs in the porous wick influenced by temperature gradient. Thus, this surface tension region should be treated as unsaturated two-phase region, in which the interstices of wick are shared by vapor and liquid at the same time. Evaporation takes place mostly on the specific interfacial area between the liquid meniscus and the vapor, which means that phase change occurs everywhere in this two-phase region. Based on this analysis, a mathematic model for the porous wick of CPL evaporator is constructed and solved numerically in the present paper, by which heat and mass transfer in vapor, two-phase and liquid regions is investigated.

2 Mathematic modeling

A segment cutting out of a flat-plate evaporator is studied through the symmetry axes of the fin and the

adjacent groove, shown in Fig. 2. To develop the mathematic model, the following assumptions are made.

1. Homogeneous and isotropic medium with no distension or contraction.
2. The effect of gravity is neglected.
3. Subject to local thermodynamics equilibrium throughout the analysis domain.
4. In unsaturated region, liquid phase and vapor phase are in funicular (continuous) state, respectively.

2.1 Single-phase region

In the single-phase regions (vapor or liquid), there is no phase change. Incompressible flows are assumed in liquid phase as well as in gas phase. The governing equations can be written as follows.

Continuum equation:

$$\frac{\partial(\varepsilon_i\rho_i)}{\partial t}+\nabla\cdot(\rho_i\vec{V}_i)=0 \tag{1}$$

Momentum equation:

$$\frac{\rho_i}{\varepsilon_i}\frac{\partial\vec{V}_i}{\partial t}+\frac{\rho_i}{\varepsilon_i^2}\left(\vec{V}_i\cdot\nabla\right)\vec{V}_i=-\nabla P_i-\frac{\mu_i}{K_i}\vec{V}_i+\frac{\mu_i}{\varepsilon_i}\nabla^2\vec{V}_i \tag{2}$$

Energy equation:

$$\bar{\rho}\bar{c}\frac{\partial T}{\partial t}+\rho_i c_i\left(\vec{V}_i\cdot\nabla\right)T=\nabla\cdot\left(k_{eff}\nabla T\right)\quad i=(l,v) \tag{3}$$

where ε is phase content, $\vec{V}$ is velocity vector, ρ is density, c is specific heat, T is temperature, P is pressure, μ is viscosity of fluid, K is permeability of porous wick, t is time, k_{eff} is effective thermal conductivity, $k_{eff}=(1-\varepsilon_s)k_i+\varepsilon_s k_s$. The subscribe v stands for vapor, l for liquid and s for solid. The heat capacity in the energy equation is defined by

$$\bar{\rho}\bar{c}=[\rho_l c_l\gamma+(1-\gamma)\rho_v c_v]\varepsilon+(1-\varepsilon)(\rho c)_s$$

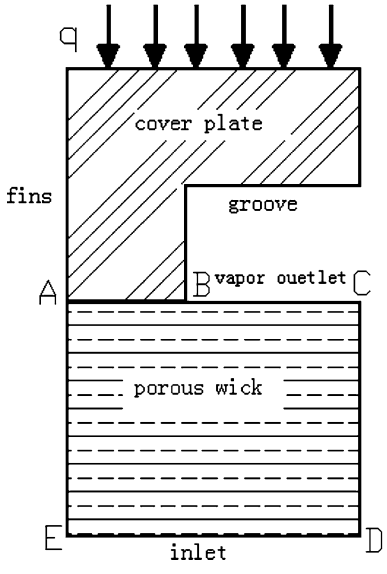

Fig. 2 Schematic of modeled CPL evaporator segment

2.2 Two-phase region

Traditionally, analyses of two-phase flow in porous media are based on the assumption that vapor and liquid phases are treated as distinct and separate fluids. The motion of each phase is described by the generalized Darcy's law in which a relative permeability is introduced to account for a decrease in effective flow cross-section due to the presence of the other phase [8]. Unfortunately, the resulting equations are not convenient for numerical solutions because the physical properties appeared are difficult to obtain and the governing differential equations are plentiful.

In what follows, we developed a model with six field variables to describe the simultaneous heat and mass migration in unsaturated porous media with phase change [9]. The field variables include temperature T, liquid content ε_l, pressure P, liquid velocity $\vec{V}_l$, vapor velocity $\vec{V}_v$ and phase-change rate $\dot{m}$. For the two dimensional model, eight variables need to be solved.

2.2.1 Continuity equations

Liquid:

$$\frac{\partial(\varepsilon_l\rho_l)}{\partial t}+\nabla\cdot(\varepsilon_l\rho_l\vec{V}_l)=-\dot{m} \tag{4}$$

Vapor:

$$\frac{\partial(\varepsilon_v\rho_v)}{\partial t}+\nabla\cdot(\varepsilon_v\rho_v\vec{V}_v)=\dot{m} \tag{5}$$

2.2.2 Momentum equations

Liquid:

$$\frac{\partial\vec{V}_l}{\partial t}+\vec{V}_l\cdot\nabla\vec{V}_l-\frac{\dot{m}}{\varepsilon_l\rho_l}\vec{V}_l=-\frac{\mu_l D_l}{\rho_l K_l}\nabla\varepsilon_l-\frac{\mu_l}{K_l\rho_l}\vec{V}_l \tag{6}$$

Vapor:

$$\frac{\partial\vec{V}_v}{\partial t}+\vec{V}_v\cdot\nabla\vec{V}_v+\frac{\dot{m}}{\varepsilon_v\rho_v}\vec{V}_v=-\frac{1}{\rho_v}\nabla p-\frac{\mu_v}{K_v\rho_v}\vec{V}_v \tag{7}$$

2.2.3 Energy equation

$$\begin{aligned}(\rho c)_m\frac{\partial T}{\partial t}&+\left((\rho c)_l\vec{V}_l+(\rho c)_v\vec{V}_v\right)\cdot\nabla T\\&+\left((\rho c)_l\vec{V}_l\cdot\nabla\varepsilon_l+(\rho c)_v\vec{V}_v\cdot\nabla\varepsilon_v\right)T\\&=\lambda_m\nabla^2T-\dot{m}\gamma+S\end{aligned} \tag{8}$$

For the above partial differential equations, some of the characteristics for the theoretical model could be discussed as follows.

1. Based on the fact of $\varepsilon = \varepsilon_s + \varepsilon_l + \varepsilon_v$, the mean physical property for specific heat capacity of porous media can be written as $(\rho\ c)_m = \varepsilon_s\ (\rho\ c)_s + \varepsilon_l\ (\rho\ c)_l + \varepsilon_v\ (\rho\ c)_v$. The apparent heat conductivity of porous media, according to the mean-weighted method, is simply defined as $\lambda_m = \varepsilon_s\ \lambda_s + \varepsilon_l\ \lambda_l + \varepsilon_v\ \lambda_v$.
2. Noting that $K_l = k_l g/\upsilon_l$ and $K_v = k_v g/\upsilon_v$, we had developed an effective formulation to calculate gaseous infiltrating conductivity K_v [10], corresponding to liquid hydraulic conductivity K_l, which can demonstrate the mechanisms of Darcy's drag resistance in terms of gaseous phase and the reaction of liquid to gaseous mixture. It could be written as

$$K_v = (1-S)^3 \left(\frac{1-\omega}{1-\omega(1-S)}\right)^{4/3} \frac{\upsilon_l}{\upsilon_v} K_l \tag{9}$$

3. According to Baggio et al. [11], the vapor pressure in a porous medium may be written as

$$p_v = p_{\text{sat}} \exp\left[\frac{-p_c M}{\rho_l R T}\right] \tag{10}$$

Where P_{sat} is saturation vapor pressure, M is molar mass of fluid (methanol for the current study), R is universal gas constant. The exponent in equation (10) has a typical magnitude 10^{-5}, and we shall hence take $p_v = p_{\text{sat}}$ in the analysis that follows.

The capillary pressure p_c, is defined as the difference between the vapor and the liquid pressures:

$$p_c = p_v - p_l \tag{11}$$

According to the Leverett function [12], we may write the capillary pressure as

$$\begin{aligned} p_c &= \delta J(s) \\ &= \delta\left[1.417(1-s) - 2.120(1-s)^2 + 1.263(1-s)^3\right] \end{aligned} \tag{12}$$

with

$$\delta = \sigma\left(\frac{\varepsilon}{\kappa}\right)^{\frac{1}{2}}$$

where σ is vapor–liquid interfacial tension, ε is porosity of porous medium.

Compared with the mathematical models for two-phase flow in porous media, for example the separate flow model (SFM) [8, 13], the present model can explain reasonable migration mechanisms and is physically meaningful. Its advantage is apparent to solve the problems involving conjugate two-phase flow with adjacent single-phase regions. When using the SFM, multiple region solutions are required due to the differences in the conservation equations for the two-phase and single-phase regions [14]. The primary numerical difficulty is associated with numerical procedures, such as moving numerical grids and/or coordinate systems. In contrast, since equations of the present model for two-phase flow strongly resembles those for single-phase transport, a unified formulation is derived that is valid throughout the entire domain, including both two-phase and single-phase regions. With such a continuum formulation, the interfaces between the regions do not require explicit consideration. The need for moving numerical grids and/or coordinate mapping is thus eliminated, as is the need for prescribing complex interfacial boundary conditions between regions internal to the domain.

2.3 Boundary conditions

The bottom boundary (D–E):

$$p_l = p_0, \quad T_l = T_0 \tag{13}$$

The symmetric boundary (A–E,C–D):

$$\frac{\partial p}{\partial x} = 0, \quad \frac{\partial T}{\partial x} = 0 \tag{14}$$

The upside boundary (A–B):

$$\frac{\partial p}{\partial y} = 0, \quad \lambda \frac{\partial T}{\partial y} = q \tag{15}$$

The upside boundary (B–C):

$$p_v = p_1, \quad \frac{\partial T}{\partial y} = 0 \tag{16}$$

where q is the system heat load (W m^{-2}).

3 Discussion

The governing equations together with the boundary conditions mentioned above are solved with the finite difference method. Noting that the pressure changes in transport process and heat and mass transfer are highly coupled, the pressure-based algorithm is principally used in the numerical formulations and computations with treating staggered grid in primitive variables and *ADI* (Alternating Direction Iterative) technique is adopted to solve the coupled linear equations. In order to ensure the convergence of calculating procedure, some technical treatments like under relaxation and error feedback are adopted.

The liquid content fields of the wick with different heat flux are shown in Fig. 3. In the calculation, we regard the region of $\varepsilon_l \le 0.01$ as saturated vapor zone. Considering an ideal steady-state condition during the operation of CPL, we first assume that the wick is separated into two regions: saturated vapor zone and unsaturated zone, and then the saturated liquid zone

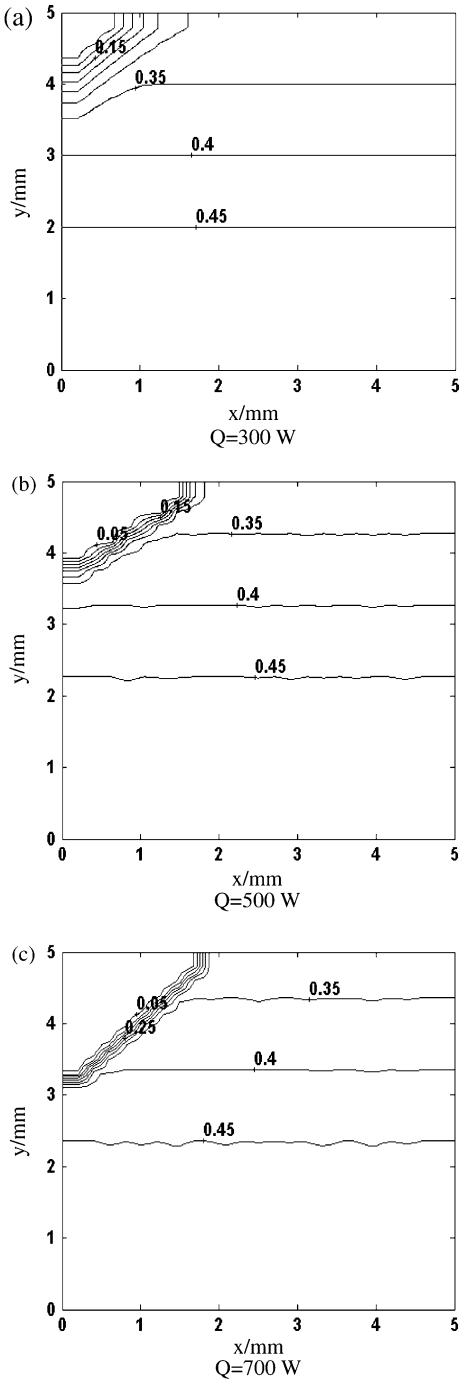

Fig. 3 Liquid content distribution in porous wick at **a** Q = 300 W; **b** Q = 500 W; **c** Q = 700 W

forms on the upper surface of liquid groove in evaporator. It is obvious in Fig. 3 that the area of vapor zone is gradually expanded when the heat flux adding on the upper fin plate increases, and the area with rather large liquid content ($\varepsilon_l \geq 0.45$) is also increased. Such a trend implies that the change of liquid content is mainly concentrated in a relatively small range between unsaturated region and vapor region, when the heat flux is increased. Since high heat flux should correspond to large mass transfer, more liquid will be delivered into the wick of evaporator with relatively high velocity, which makes the liquid content in the bottom of the wick become large. When the liquid is transported into the two-phase zone the surface tension becomes weak, and with the increases in temperature gradient, surface tension decreases quickly. This may account for why the area of vapor zone becomes bigger at higher heat flux. According to the trend of liquid content field showed in Fig. 3, we just can say that the usual treatment of liquid-vapor phase change as a front surface with zero thickness may be only suitable for certain situations with rather large heat flux.

The temperature fields of the wick at different heat flux are showed in Fig. 4. It can be seen that there exists no clear boundary between two-phase region and vapor region like the situation in the liquid content fields. But the large temperature gradient is concentrated in the vapor zone, and also in the two-phase zone near the vapor zone, i.e., low and moderate liquid content zones. When such an area becomes larger, the temperature arises more quickly, as shown in Fig. 4c. As the temperature changes very slightly in the bottom zone, the liquid content changes very slightly in the same region. Compared to the numerical results shown in Figus [15], it can be found that the area with high temperature is much smaller when the unsaturated region is considered, which is more reasonable.

Patterns of evaporation rate in the wick with different heat flux are shown in Fig. 5. The large temperature gradients of two-phase zone, apparent in Fig. 4, are mapped into high evaporation rate in Fig.5. That is, the area where the phase change occurs intensely is very narrow and locates at the upper end of the two-phase zone. It can also be found that there is no obvious phase change in the single-phase zone and even in the area of two-phase zone that the liquid content change is little. Moreover, with an increase of heat flux the area of strong evaporation narrows down, and the magnitude of evaporation rate increases significantly. Such a result challenges the conventional saturated model [2, 3, 15] in which the fluid phase change occurs only at a zero thickness interface between vapor zone and liquid zone. The experimental results of Udell [5] also show that there exists a very thin evaporation zone, which tallies with the results of this paper.

It can be seen that the convective movement inside the vapor zone, as well as high-liquid-content zone, is very weak. The mass transfer mostly takes place in the area of large liquid content. This peculiarity is caused by the fact that in the model of single-phase region the interaction of liquid and vapor is absent, and the driven force to make the fluid flow is just the evaporation at interface.

The velocity field and pressure distribution of the vapor and the liquid are presented in Figs. 6 and 7 respectively. As indicated in Fig. 5a, the vapor velocity is rather low in the saturated vapor zone ($\varepsilon_l \leq 0.01$), and is lower in the high-liquid-content zone (the approximate liquid-saturated zone, $\varepsilon_l \geq 0.45$). The mass

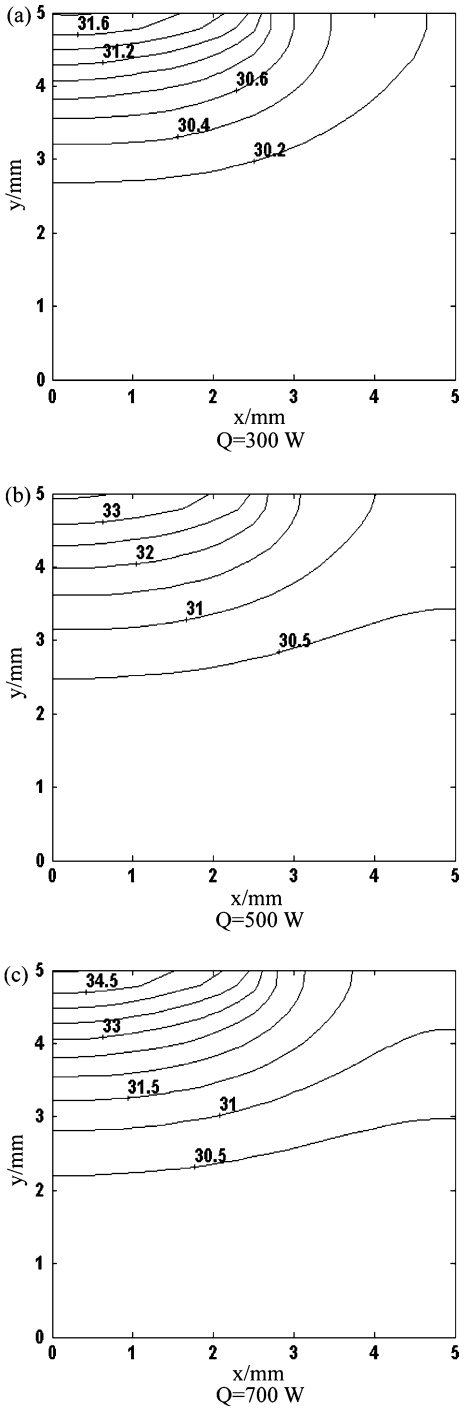

Fig. 4 Temperature field in porous wick at **a** Q = 300 W; **b** Q = 500 W; **c** Q = 700 W

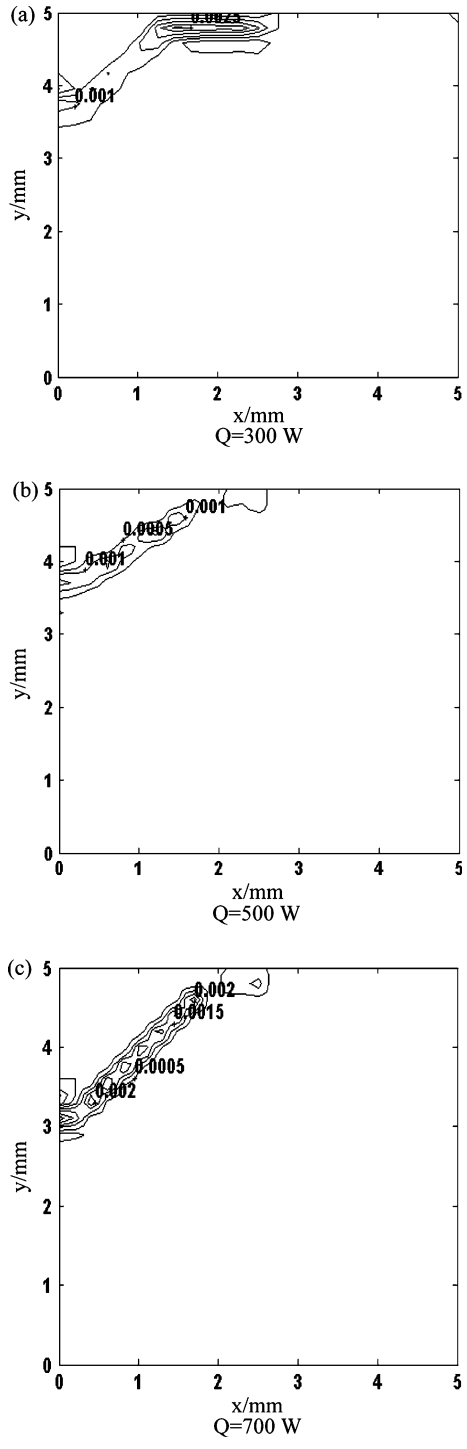

Fig. 5 Patterns of evaporation rate in porous wick at **a** Q = 300 W; **b** Q = 500 W; **c** Q = 700 W

transfer mostly takes place in the area of large liquid content gradients. This phenomena is related to many factors, including the boundary effect of vapor flow, the geometry factor of the fluid flow line, the vapor outlet direction and the mass continuity and so on. Corresponding to the vapor velocity distribution, the liquid convective movement is intense in the high-liquid-content area and weak in the area of intensity-evaporation zone, as shown in Fig. 7.

4 Conclusion

A three-region model is developed to describe the transport process in capillary pumped loop. Special attention is paid on the unsaturated porous medium evaporating region, and a six-field model is developed to describe the physical process. Since the equations are

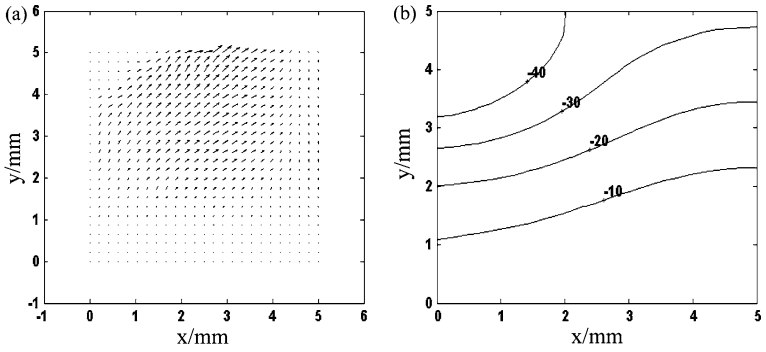

Fig. 6 Vapor velocity field (**a**) and pressure distribution (**b**) in porous wick at Q = 500 W

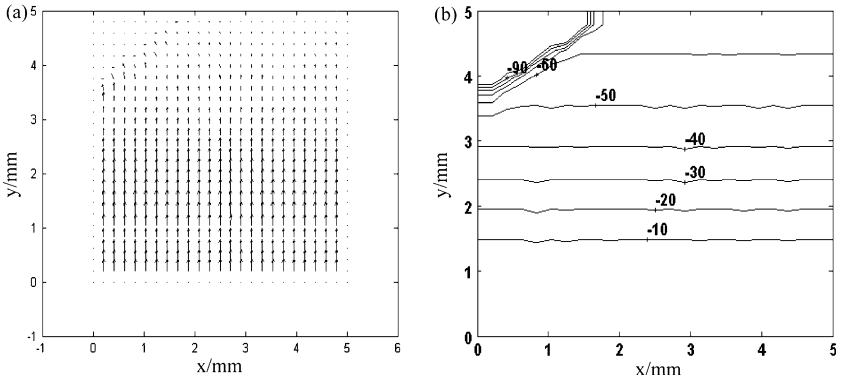

Fig. 7 Liquid velocity field (**a**) and pressure distribution (**b**) in porous wick at Q = 500 W

general and are of the same form as those in single-phase transport in porous medium, they are quite convenient for numerical simulation of multi-region problem.

Numerical results show that the change of liquid content in the porous wick of evaporator of CPL is obviously. This implies that the phase change region between two single-phase regions should be treated as a liquid-unsaturated region. The variation of liquid content is more and more concentrated in a narrow range with the heat load on the evaporator increased. This indicates a trend that the thickness of unsaturated region may reduce as heat load increase.

Acknowledgements The current work is financially supported by the National Key Basic Research Development Program of China (No.G2000026303).

References

1. Cao Y, Faghri A (1994) Conjugate analysis of a flat-plate type evaporator for capillary pumped loops with three-dimensional vapor flow in the groove. Int J Heat Mass Transfer 37(9):401–409
2. Cao Y, Faghri A (1994) Analytical solutions of flow and heat transfer in a porous structure with partial heating and evaporation on the upper surface. Int J Heat and Mass Transfer 37(10):1525–1553
3. Khrustalev D, Faghri A (1995) Heat transfer in the inverted meniscus type evaporator at high heat fluxes. Int J Heat Mass Transfer 38:(16)3091–3101
4. Su HJ (1981) Heat transfer in porous media with fluid phase change, Ph.D. thesis, University of California, Berkeley
5. Udell KS (1983) Heat transfer in porous media heated from above with evaporation, condensation, and capillary effects, ASME. J Heat Transfer 105:485–492
6. Zhao TS, Cheng P, Wang CY (2000) Buoyancy-induced flows and phase-change heat transfer in a vertical capillary structure with symmetric heating. Chem Eng Sci 55:2653–2661
7. Zhao TS, Liao Q (2000) On capillary-driven flow and phase-change heat transfer in a porous structure heated by a finned surface: measurements and modeling. Int J Heat Mass Transfer 43:1141–1155
8. Bear J (1972) Dynamics of fluids in porous media. Elsevier, New York
9. Liu W, Huang XM, Riffat SB (2003) Heat and mass transfer with phase change in a rectangular enclosure packed with unsaturated porous material. Heat and Mass Transfer 39:223–230
10. Liu W, Shen S, Riffat SB (2002) Heat transfer and phase change of liquid in an inclined enclosure packed with unsaturated porous media. Int J Heat and Mass Transfer 45:5209–5219
11. Baggio P, Bonacina C, Schrefler BA (1997) Some considerations on modeling heat and mass transfer in porous media. Transp Porous Media 28:233–251
12. Leverett MC (1941) Capillary behavior in porous solids. AIME Trans 142:152–169
13. Scheidegger AE (1974) The physics of flow through porous media (3rd edn). University of Toronto Press, Toronto
14. Ranesh PS, Torrence KE, Numerical algorithm for problems involving boiling and natural convection in porous materials. Numer Heat Transfer Part B Fundam 17:1–24
15. Figus C, Le Bray Y, Bories S et al (1999) Heat and mass transfer with phase change in a porous structure partially heated: continuum model and pore network simulations. Int J Heat Mass Transfer 42:2557–2569